J. Fluid Mech. (1983), *vol.* 130, *pp.* 91–108
Printed in Great Britain

A study of the spanwise structure of coherent eddies in the viscous wall region

By C. NIKOLAIDES, K. K. LAU† AND T. J. HANRATTY
University of Illinois, Urbana, Illinois

(Received 14 September 1981 and in revised form 4 August 1982)

Simultaneous measurements of the longitudinal and spanwise components s_x and s_z of the fluctuating velocity gradient at the wall of a pipe and the fluctuating velocity u and w at various distances from the wall have been analysed in order to provide information on the origin of flow-oriented wall eddies. Special conditional-averaging techniques, which use multiprobe measurements, are developed to capture the wall structures as they evolve in both space and time. It is found that wall eddies of wavelength $\lambda^+ \approx 100$, detected from measured patterns of $s_z(z)$, are closely related to spanwise variations of the velocity at $y^+ = 20$ and 40. Analysis of measurements from probes arranged in the direction of the mean flow supports the notion that the wall structures result from the propagation of spanwise disturbances of the velocity at some distance from the wall, both downstream and towards the wall. A flow model, different from vortex models hypothesized by previous investigators, is proposed to account for the relation of flow phenomena in the viscous wall region to the low-speed wall streaks.

1. Introduction

Visual investigations made by Hama (Corrsin 1957), Kline & Runstadler (1959) and Kline *et al.* (1967) reveal the existence of low-speed streamwise filaments at the wall that are elongated in the direction of flow and that have an average spacing of $\lambda^+ = 100$. These coherent structures have received considerable attention because of their possible importance in determining the transfer of energy from the mean flow to the turbulence. Yet the details of the motion in them and their origin are still not completely understood. This paper is aimed at providing support for the notion that they can be viewed as secondary flows associated with velocity fluctuations at the edge of the viscous wall region $30 \leqslant y_0^+ \leqslant 50$. In particular it reports the results of experiments in which the occurrence of strong coherent structures at the wall is related to transverse velocity fluctuations at different y^+.

Bakewell & Lumley (1967) suggested that the wall streaks result from counter-rotating pairs of eddies homogeneous in the flow direction. Sirkar & Hanratty (1970*a*) also suggested that the flow in the wall region is dominated by a secondary pattern homogeneous in the flow direction that is of the type shown in figure 1 (*a*). According to the model, the streaks observed when dye is injected from a wall slot result from the sweeping action of the secondary flow in the transverse direction close to the wall.

Fortuna and Hanratty (Fortuna 1971; Chorn, Hatziavramidis & Hanratty 1977) assumed that, on average, the streamlines in the secondary flow have the shape shown in figure 1 (*a*), and used a pseudosteady-state assumption to calculate the streamwise

† Present address: Gulf Research, Pittsburgh, Pennsylvania.

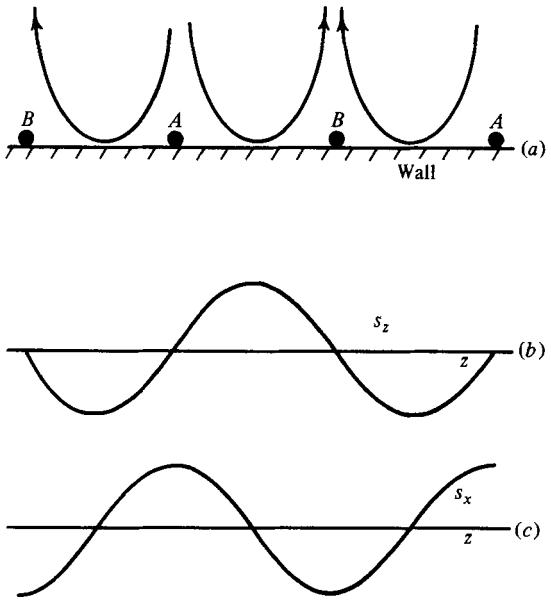

FIGURE 1. Idealized coherent eddy structure.

velocity component. They pictured the secondary flow to bring high-momentum fluid to the wall at A, to exchange momentum with the wall as it moved fluid in the transverse direction from A to B, and to remove low-momentum fluid from the wall at B. According to this picture, the streamwise s_x and spanwise s_z components of the velocity gradient at the wall should have the phase relation shown in figures 1 (b, c).

Hatziavramidis & Hanratty (1979) undertook a computational study to explore how the viscous wall region would respond to transverse velocity fluctuations at its outer boundary $y_0^+ \approx 30$–40. The basic model was similar to the one used by Fortuna (1971), but it was recognized that his pseudosteady-state assumption overlooks important aspects of the flow. The flow field in the viscous wall region was pictured to be coherent and to be associated with flow deviations in a well-mixed outer region. The transverse flow at $y_0^+ \approx 30$–40 was taken as $w = w_L \sin(2\pi z/\lambda) \cos(2\pi t/T_B)$, where λ is the spacing of the dye streaks, T_B the period between bursts, and w_L a constant. Good agreement was obtained between the calculated flow field and experimental results, especially for $y^+ < 15$. Of particular importance to the work reported in this paper is the prediction of phase changes and lag times between the velocity gradient at the wall and the fluid velocity at different distances from the wall.

The initial motivation for the model in figure 1 (a) was provided by measurements of s_x and s_z obtained by Sirkar & Hanratty (1970b) by studying the mass-transfer rates to a pair of rectangular electrodes mounted in a chevron arrangement flush with the wall. The results of these experiments showed that the transverse flow at the wall is quite large, s_z being about $0.1S_x$.

Lee, Eckelmann & Hanratty (1974) used an array of electrode pairs to measure s_x and s_z simultaneously at a number of locations on the wall. Their experiments support the existence of a secondary flow pattern of the type visualized by Sirkar & Hanratty (1970a) and the proposal of Fortuna (1971) regarding the influence of this secondary flow on the streamwise velocity fluctuations. In particular it was found that the s_z variation in the spanwise direction can, on average, be adquately described by a sinusoidal variation of the type shown in figure 1 (b). It was also shown that the

s_z pattern is accompanied by a spatial variation of s_x that is out of phase by $\frac{1}{4}\lambda$. Their measurements of λ are in good agreement with results of the visual studies, cited above.

These results of Lee *et al.* established the patterns of s_x and s_z at the wall which are associated with the wall eddies, but left unanswered the question of how well, if at all, events at the wall are related to phenomena occurring at distances away from the wall. For this purpose, conditionally averaged velocity measurements are needed which reflect in a direct way the relation of the velocity field to changes in the eddy structure and which give information on how the eddy structure and velocity field evolve in time. One way of doing this would be to combine instrumental measurements of the velocity field with dye pattern measurements. We have taken a different approach in two recent experiments in our laboratory performed by Hogenes (1979; Hogenes & Hanratty 1982) and by Lau (1980).

Measurements of s_z at a number of z-locations are compared with the pattern shown in figure 1 (*b*) to determine whether a strong eddy exists. Probes that are mass-transfer analogues of the hot-film anemometer are located over the centre of this array, defined as $z = 0$, in order to measure properties of the velocity field. Four aspects of strong wall eddies are defined. Positive or negative values of $\mathrm{d}s_z/\mathrm{d}z$ at $z = 0$ indicate respectively that a strong inflow or outflow would be sampled by the fluid probes. Maxima or minima in $s_z(z)$ at a fixed time indicate strong positive or negative spanwise flows, and, on average, a coupled inflow and outflow at distances of $\Delta z^+ \approx 25$ from the centre of the wall-probe array.

In a previous paper (Hogenes & Hanratty 1982) the influence of these eddies, defined in terms of the $s_z(z)$ pattern, on the axial velocity component was examined by studying how the $s_x(z)$ pattern and the streamwise velocity profile at $z = 0$ are associated with changes in the eddy pattern. In this paper the relation of wall patterns to transverse velocity fluctuations in the fluid is studied by determining the relation of the transverse velocity at different values of x, y and z to changes in the eddy structure detected by the multiple wall probes.

Similar investigations have also been carried out by Blackwelder & Eckelmann (1978, 1979) and Kreplin & Eckelmann (1979). Blackwelder & Eckelmann studied the spanwise structure of the bursting phenomenon. They located a fluid probe, sensitive to streamwise velocity fluctuations, at $y^+ = 15$ in order to detect bursts and conditionally averaged measurements of s_x and s_z at one wall location as well as measurements of u and w at a fixed distance from the wall. Their detection scheme was a variable-interval time-averaging (V.I.T.A.) scheme that had been used by Kaplan & Laufer (1969) to study the intermittently turbulent region of a boundary layer. They concluded that the 'bursting' phenomenon is associated with pairs of counterrotating vortices that seem to 'pump' fluid away from the wall, thus forming a low-speed streak. They also found that the streamwise momentum defect region is long and narrow, and that the velocity defect is terminated by a strong acceleration followed by a high-speed region.

Kreplin & Eckelmann (1979) investigated the propagation of perturbations in the wall region of a turbulent shear flow. They used a movable V-probe to measure the streamwise and spanwise components of the velocity at a certain distance from the wall. They also used a V-probe mounted on a wall plug at a wall distance of $y^+ = 2.3$ in order to measure the same components close to the wall. The movable V-probe was located at $x^+ = 0$ and $y^+ = 5$, 10, 20, 40, and the wall plug was positioned at $x^+ = -108$, 0 and $+144$. From the correlation measurements Kreplin & Eckelmann deduced that the wall region is dominated by pairs of inclined counterrotating

streamwise vortices. The average spanwise separation of their centres is about $z^+ \approx 50$, and the length of the vortices was estimated to be $x^+ \approx 1200$. As these vortices are convected downstream the angle of their plane of rotation was pictured to decrease, and the average minimum distance of the vortex centre from the wall was estimated to be $y^+ \approx 30$.

An essential difference between the present work and previous works is the use of multiple wall probes to detect the wall structures. The difficulty with detecting the wall structures lies in the fact that they evolve both in space and time, and the use of a single probe cannot provide information regarding their spatial development. In addition, the use of multiple wall probes aligned in the flow and spanwise directions along with a fluid probe at a fixed distance from the wall allowed us to extend the range of correlation measurements presented in the literature (Kreplin & Eckelmann 1979).

2. Experimental methods

The experimental results analysed in this paper were obtained by Lau (1980) in a 20 cm flow loop built by Sirkar (1969). Details about its construction and operation were published in previous papers (Sirkar & Hanratty 1970*a*, *b*).

A drawing of the test section is shown in figure 2. It was made from an acrylic pipe, with an internal diameter of 20 cm and a length of 2 m. The fluid probe sensors were manufactured by TSI Inc. Each pair was separated by a distance of 1 mm and was constructed from elements with a length of 1 mm and a diameter of 0.05 mm. Forty pairs of multiple V-shaped wall electrodes were aligned perpendicular to the mean flow direction. Only nine pairs were used in this work. Single V-shaped probes were located at various positions in the streamwise direction. A schematic diagram of the arrangement of the measuring sensors is shown in figure 3.

All outputs from the electrode circuit were adjusted to have values between ± 5 V. This was necessary because all analog signals were digitalized by an A/D converter having a resolution of only 16 bits. The A/D converter was controlled by an IBM 1800 computer. Before digitalization, the signals were filtered by a fourth-order low-pass Butterworth filter with a cutoff frequency of 15 Hz, which corresponds to a dimensionless frequency of $n^+ = 1$. The sampling frequency was 20 Hz and the sampling time 400 s. The data were stored in integer form in magnetic discs. Each disc has a capacity of approximately 400000 words. These raw data were then transferred to magnetic tapes and analysed in a CDC Cyber computer.

Both the wall and fluid probes were electrodes operated under conditions that the current flowing in the circuit is directly proportional to the rate of mass transfer to the electrodes. The electrolyte used in the experiments was a solution of iodine in potassium iodide with a concentration of 0.1 M-KI and 0.001 M-I_2. Details regarding these techniques have been given in a number of previous papers from this laboratory (see e.g. Lee *et al.* 1974; Hogenes & Hanratty 1982).

The mass-transfer rates to the wall electrodes were related to s_x and s_z through analytical expressions developed by Sirkar & Hanratty (1970*b*). The relation of the mass-transfer rates to fluid probes to velocity components U and w was obtained empirically using the following expressions:

$$U = A(V_{1\ell} + V_{2\ell}),$$

$$w = A(V_{1\ell} - V_{2\ell}),$$

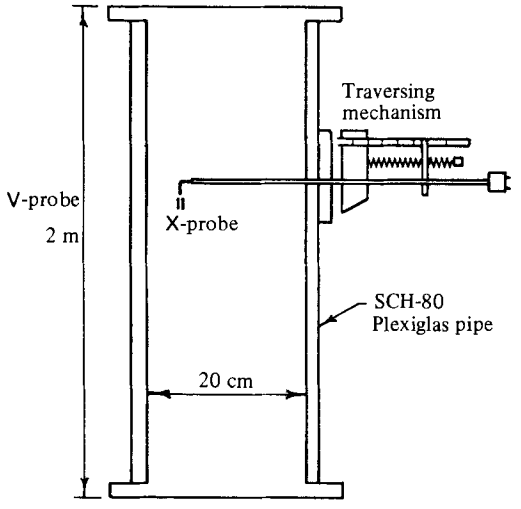

FIGURE 2. Design of test section.

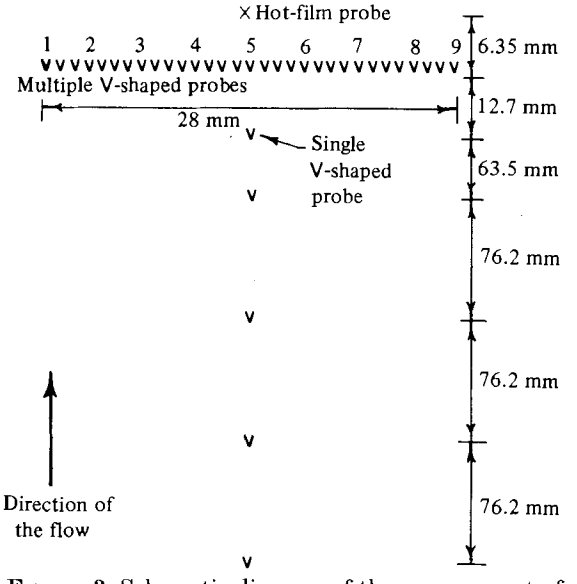

FIGURE 3. Schematic diagram of the arrangement of sensors.

where A is a constant and $V_{1\ell}$, $V_{2\ell}$ are the linearized voltage outputs from sensors 1 and 2; i.e. $V_{1\ell} = E_1^\beta$, $V_{2\ell} = E_2^\beta$, where E_1, E_2 are the voltage drops across the respective resistors. The calibration runs were carried out at the centre of the pipe at different Reynolds numbers. The value of β obtained is in agreement with the one measured by Hogenes (1979). It was found that, in order to ensure that $uw \approx 0$ and $w^3 \approx 0$, the angle formed by flow direction and the line that bisects the sensor angle had to be readjusted approximately 2°.

3. Conditional-sampling scheme

The development of an effective detection scheme requires knowledge of the general and specific features of the patterns that are to be conditionally sampled.

In the case of the wall region of a bounded turbulent shear flow the situation is

quite complicated. The wall structures evolve both in space and time, and this has to be accounted for in the sampling procedure. Observations of the instantaneous signatures of the wall eddies, as characterized by the spanwise variation of s_z, show a number of interesting characteristics. There are periods of time that the wall is dominated by eddies that grow in size and wander back and forth in the spanwise direction. There are also time intervals during which nothing spectacular occurs close to the wall.

Hogenes (1979; Hogenes & Hanratty 1982) used the idealized sinusoidal variation of s_z shown in figure 1 (*b*) to define four distinct eddy patterns related to the midpoint *MP* of the wall probe array. For two of them, the s_z profile exhibits a maximum or a minimum above *MP*, and, for the remaining two, it shows a zero-crossing at *MP* with either a negative or a positive slope.

We have adopted this same classification even though it is an extremely simplified approach to the problem. Since the patterns shift in the spanwise direction and the wavelength varies in time, the above-selected eddy patterns represent limiting modes of the spanwise variation of s_z. The selection of the centre of the probe array as a reference point for the classification of the eddy patterns is dictated by the fact that the fluid probe is located directly above *MP*.

In order to measure the strength of the eddy pattern the following function was employed:

$$\hat{S}_{dk} = \sum_{i=1}^{9} \left| s_{zi}(t_k) \right| - \left| \sum_{i=1}^{9} s_{zi}(t_k) \right|,$$

where i refers to the ith probe, k to the instant t_k in the data set, and s_{zi} is made dimensionless using $(\overline{s_z^2})^{\frac{1}{2}}$. It is easily seen that $\hat{S}_{dk} \geqslant 0$ for all t_k and that $\hat{S}_{dk} = 0$ when all the s_{zi} are either positive or negative. An ideal eddy pattern similar to the one shown in figure 1 (*a*) with an amplitude equal to $(\overline{s_z^2})^{\frac{1}{2}} \approx 0.11$ and a wavelength of $\lambda^+ \approx 100$ would give a value of $\hat{S}_{dk}$ approximately equal to 4.7.

The function $\hat{S}_{dk}$ is plotted in figure 4 for 1000 data ponts or $\frac{1}{8}$ of the data set. One can easily identify periods of activity associated with the peaks of $\hat{S}_{dk}$ and periods of relative quiet when $\hat{S}_{dk}$ decreases towards zero. If a threshold level $\bar{S}_d$ is applied to $\hat{S}_{dk}$, then for the time instants t_k that $\hat{S}_{dk} \geqslant \bar{S}_d$ a strong eddy patter, similar to the one in figure 1 (*a*), occurs over the wall-probe array.

In order to be able to identify this eddy pattern with one of the four limiting modes of the s_z profile defined by Hogenes, additional information is needed. For this purpose, the product $P_k = s_{z4}(t_k)\ s_{z6}(t_k)$ is formed using the signals from probes 4 and 6 that are at equal distances from the middle probe 5 of the wall-probe array. When $P_k > 0$, the sign of $s_{z5}(t_k)$ is checked, and, when $P_k < 0$, the difference $D_k = s_{z4}(t_k) - s_{z6}(t_k)$ is computed.

The objective of the scheme is to relax the stringent requirements, used in earlier efforts from this laboratory, of having a zero-crossing of s_z or a maximum (minimum) exactly at probe 5. Four different aspects of the eddy motion are then recognized at probe 5:

(1) $P_k > 0$, $s_{z5}(t_k) > 0$ positive transverse flow (PTF);
(2) $P_k > 0$, $s_{z5}(t_k) < 0$ negative transverse flow (NTF);
(3) $P_k < 0$, $D_k > 0$ outflow;
(4) $P_k < 0$, $D_k < 0$ inflow.

For cases (1) and (2) when also $s_{z4}(t_k)\ s_{z5}(t_k) < 0$ (or $s_{z6}(t_k)\ s_{z5}(t_k) < 0$), the smallest resolvable wavelength is detected.

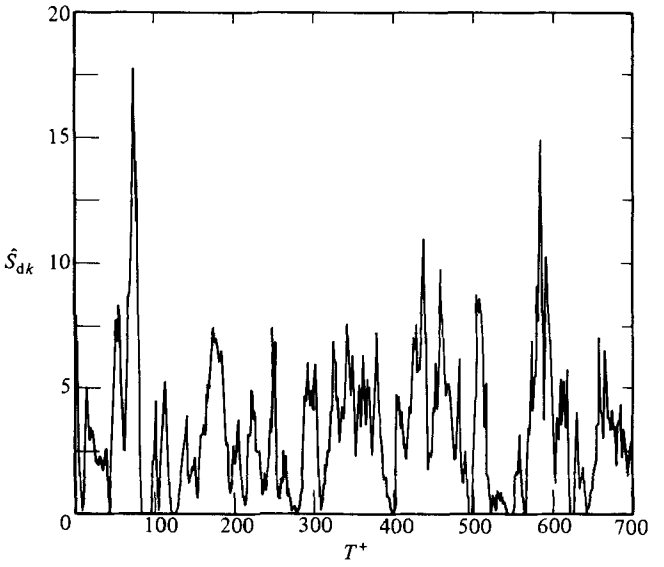

FIGURE 4. Plot of the detection function $\hat{S}_{dk}$ versus T^+.

It is clear that $\hat{S}_{dk}$ defines a strong event and (1)–(4) distinguish the type of eddy pattern. The function $\hat{S}_{dk}$ is similar to the one used by Kovasznay, Kibens & Blackwelder (1970) as a turbulence detector. The parameter $\hat{S}_{dk}$ detects periods of time when the wall is dominated by strong eddy patterns and time intervals when the wall activity subsides. It is to be noted that $\hat{S}_{dk}$ is not used to define any reference time for the conditional-averaging procedure. Time zero for the averaging scheme is defined as the midpoint of the duration time of each pattern.

If, for example, $P_k > 0$ and $s_{z5}(t_k) > 0$ for $t_m \leqslant t_k \leqslant t_n$ and $\hat{S}_{dl} \geqslant \tilde{S}_d$ for some t_l, where $t_m \leqslant t_l \leqslant t_n$ and $\tilde{S}_d$ is a suitable threshold level, then a strong positive transverse flow occurs over the wall-probe array and zero time is selected as $t_0 = \frac{1}{2}(t_m + t_n)$.

For an idealized eddy pattern $\hat{S}_{dk} \approx 4.7$, as mentioned before. The average value

$$\hat{S}_{d\,av} = K^{-1} \sum_{k=1}^{K} \hat{S}_{dk} \approx 4$$

for all the experimental runs (K is the total number of data points). It seems reasonable to select a threshold level $\tilde{S}_d$ that is close to the above two characteristic values of the detection function $\hat{S}_{dk}$. The effect of varying $\tilde{S}_d$ will be discussed later.

An example of how the conditional sampling scheme works is shown in figure 5. It is seen that $P_k < 0$, $D_k < 0$ for $4.6 < t^+ < 13.3$ and $P_k > 0$, $s_{z5} < 0$ for $13.3 < t^+ < 28$, where $t^+ = 0$ is some arbitrary time instant. If $\tilde{S}_d = 4$, then $\hat{S}_{dk} > \tilde{S}_d$ for $8.5 < t^+ < 28.8$, and the scheme would detect an inflow followed by a negative transverse flow. Time zero for the inflow eddy pattern would be selected as $t_0^+ = 8.95$ and for the NTF pattern $t_0^+ = 20.65$.

In previous work from this laboratory, Hogenes constructed a scheme to analyse multiple-wall-probe measurements which is quite different from what is presented above. Detection coefficients that are sensitive to the symmetry or antisymmetry of the eddy patterns, as characterized by the s_z variation, were used to conditionally sample strong eddies at the wall. The time instant that a detection coefficient attained its maximum value was defined as zero time.

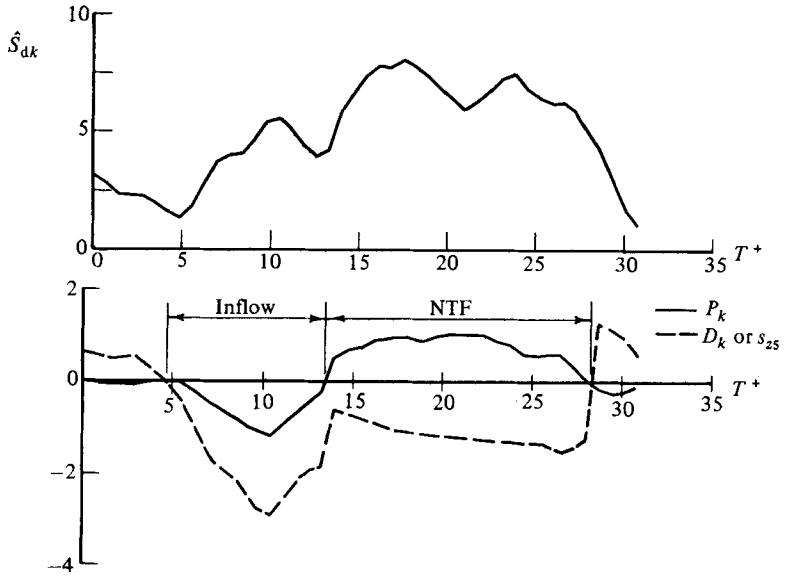

FIGURE 5. Example of how the detection scheme works.

The scheme described in the present work is considered to be an improvement over the one used previously by Hogenes for the following reasons. The strength and type of pattern are recognized by two independent processes. The use of conditions (1)–(4) eliminates the effect of the 'shifting' of the eddy pattern and defines a reference time based on more than one time instant. The use of one threshold level on $\hat{S}_{dk}$ gives equal weight to all four types of eddy motion.

Hogenes developed extra detection algorithms to study the temporal succession of the eddy patterns. This is avoided in the present detection scheme. Once the various modes of the s_z signature are isolated in the time axis it is easy to explore their temporal relation.

Some comments are also necessary regarding the number of events included in the conditional averaging procedure. When a positive (or negative) transverse flow occurs over *MP*, an outflow takes place at a distance of $\Delta z^+ \approx 25$ from *MP*. So it is seen that an outflow is associated with three of the four limiting modes of the s_z variation, as discussed above. If an attempt is made to relate outflows to the observed 'bursts' (Rundstadler, Kline & Reynolds 1963) one should recognize that not all outflows might eventually evolve into a burst. According to measurements by Kline *et al.* (1967), the frequency of streak breakup per unit of span made dimensionless with wall parameters is approximately equal to 10^{-4} for flows with negligible pressure gradient. For a spanwise length of $\lambda^+ < 100$ the bursting frequency is thus $10^{-4} \times 100 = 0.01$.

Since the time duration of the experiments described in this study is $T^+ = 5600$ the number of bursts over the wall probe array should be equal to $5600 \times 0.01 = 56$. One would, therefore, expect that the sum of outflows, positive and negative transverse flows detected by the detection algorithm would at least be equal to 56.

These types of considerations provide an independent check on the number of the events selected for the averaging process. They could also help in constructing a technique for measuring the 'bursting' frequency.

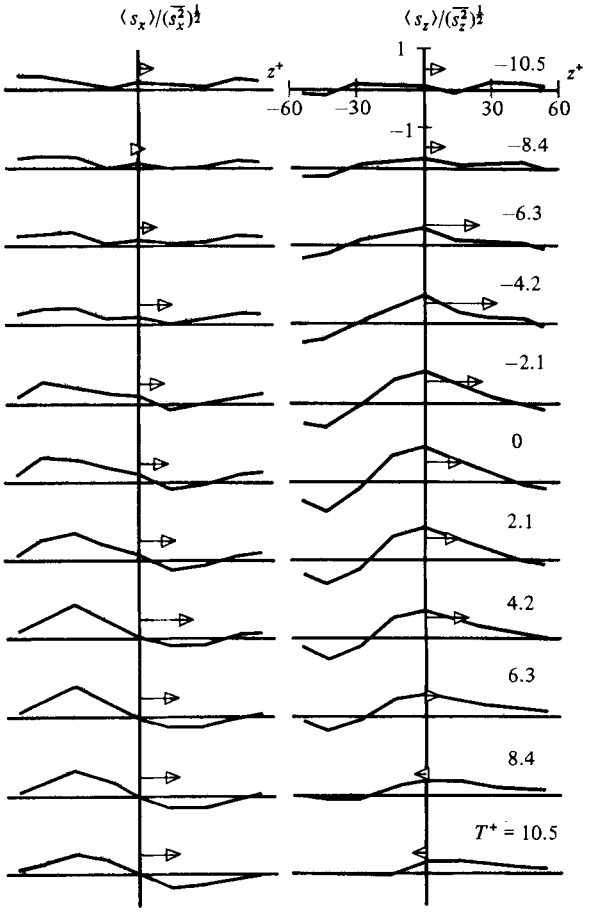

FIGURE 6. Conditionally averaged data for positive transverse flows at the wall; the fluid probe at $y^+ = 20$. Arrow length of +60 indicates $\langle w \rangle / (\overline{w^2})^{\frac{1}{2}}$ or $\langle u \rangle / (\overline{u^2})^{\frac{1}{2}}$ equal to +1.

4. Results

4.1. *Relation of wall patterns to transverse velocity fluctuations in the fluid*

Figures 6 and 7 show results of experiments in which the s_z patterns detected at the wall are associated with transverse velocity fluctuations in the fluid at $y^+ = 20, 40$. The fluid probe was located at $\Delta x^+ \approx 25$, as is shown in figure 3. This separation causes only a small delay time of $T^+ \approx 1.5$ in detecting events at $x^+ \approx 0$ at the same y^+. Lag times between events at the fluid probe and the array of wall probes therefore can be associated primarily with the separation normal to the wall.

The s_z patterns shown in figures 6 and 7 were conditionally averaged for a positive transverse flow at $z^+ = 0$ using condition (1) with $\tilde{S}_d = 4$. Data points were actually taken every $\Delta T^+ = 0.7$ but the results are presented every $\Delta T^+ = 2.1$. Fifty events were averaged for $y^+ = 40$ and 49 events for $y^+ = 20$. The effect of the threshold level $\tilde{S}_d$ on the number of events obtained is shown in table 1. It is seen that even for large threshold levels one obtains a sufficient number of events according to arguments presented in §3.

As seen in the run with the fluid probe at $y^+ = 20$, an s_z profile with a maximum at $z^+ = 0$ and a wavelength of $\lambda^+ \approx 100$ starts to develop at $T^+ \approx -9.1$, reaches its maximum amplitude of $1.0(\overline{s_z^2})^{\frac{1}{2}}$ at $T^+ = 0.7$ and dies out at $T^+ = 9.8$. It is to be noted

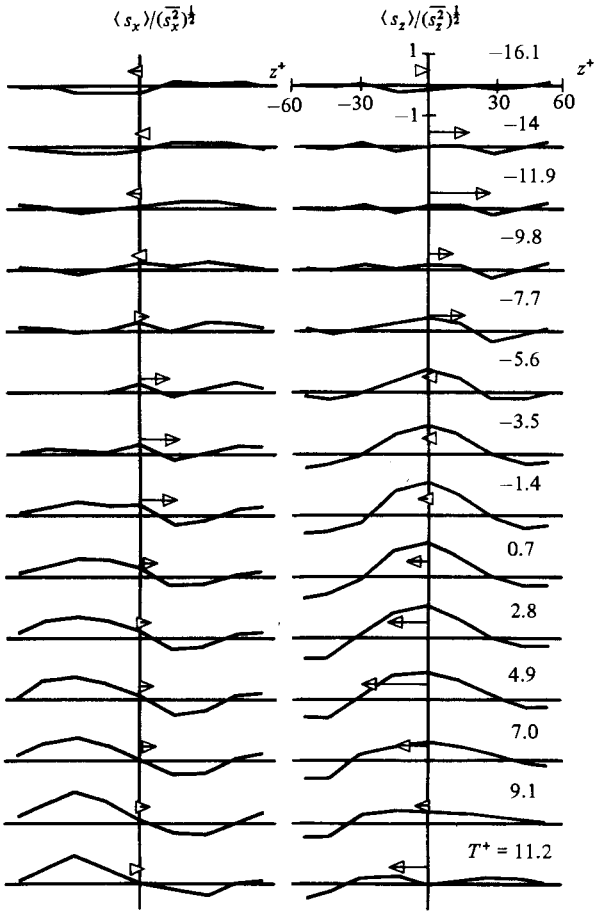

FIGURE 7. Conditionally averaged data for positive transverse flows at the wall; the fluid probe at $y^+ = 40$. Arrow length of +60 indicates $\langle w \rangle/(\overline{w^2})^{\frac{1}{2}}$ or $\langle u \rangle/(\overline{u^2})^{\frac{1}{2}}$ equal to +1.

$\tilde{S}_d$	No. of PTFs	No. of NTFs	No. of outflows
3	59	62	59
4	50	56	52
5	43	42	44
6	37	38	38

TABLE 1. The effect of $\tilde{S}_d$ on the number of detected events; fluid probe at $y^+ = 40$

that the s_x profiles lag the development of the s_z profiles by $\Delta T^+ \approx 7.7$. These are sine waves with a maximum at $z^+ = -25$ and a minimum at $z^+ = 25$, corresponding to coupled inflows and outflows at these locations.

The arrows in figures 6 and 7 represent the magnitude and direction of the conditionally averaged z and x velocity components at $y^+ = 20$ or 40. An arrow extending to $z^+ = 60$ indicates a value of $\langle w \rangle/(\overline{w^2})^{\frac{1}{2}}$ or of $\langle u \rangle/(\overline{u^2})^{\frac{1}{2}}$ of +1. An arrow extending to $z^+ = -60$ indicates a ratio of the conditionally averaged to the root-mean-square fluctuating velocity component of minus one. It is noted that positive transverse flows at the wall are associated with positive transverse flows at $y^+ = 20$. The transverse flow at $y^+ = 20$ attains a maximum value of $0.6(\overline{w^2})^{\frac{1}{2}}$ at

$T^+ = -3.5$, indicating that the flow at the wall lags that at $y^+ = 20$. This is consistent with the finding by Hatziavramidis & Hanratty (1979) and by Kreplin & Eckelmann (1979) that it takes a finite time for disturbances in the outer flow to propagate to the wall.

The conditionally averaged s_x and s_z profiles obtained in the run with the probe at $y^+ = 40$ are very similar to those shown in figure 7, as would be expected if the experiments were reproducible. The arrows in figure 7 represent the magnitude and direction of the conditionally averaged z and x velocity components at $y^+ = 40$. It is noted that at $y^+ = 40$ the conditionally averaged transverse component is positive before the flow at the wall starts to build up and has a maximum value of $0.5(\overline{w^2})^{\frac{1}{2}}$ at $T^+ = -12.6$. Around $T^+ =$ where s_z reaches its maximum amplitude of $1.15(\overline{s_z^2})^{\frac{1}{2}}$, the conditionally averaged w changes sign. We interpret these results as indicating that the flow at the wall is caused by transverse velocity fluctuations of the same sign at $y^+ = 40$. Because it take a finite time for disturbances at $y^+ = 40$ to propagate to the wall the flow at $y^+ = 40$ has, on average, changed direction when activity at the wall is a maximum.

Kreplin & Eckelmann (1979) made measurements of the correlation between s_z and the transverse component of the velocity at $y^+ = 5$, 10, 20, 40 and at $\Delta x^+ = -108$, 0, $+144$. The results shown in figure 7 agree with their measurements in that they found that disturbances propagate to the wall and that the correlations at $y^+ = 40$ are negative. However, Kreplin & Eckelmann interpreted their results differently. As mentioned in §1, they deduced that the wall region is dominated by pairs of inclined, counterrotating streamwise vortices with an average transverse separation of their centres of about $z^+ \approx 50$ and a length of $x^+ \approx 1200$. They envisioned that as these vortices are convected downstream the angle of their plane of rotation decreases and that the average minimum distance of the vortex centre from the wall is $y^+ \approx 30$.

4.2. *Streamwise variation of the eddy structure*

Correlations calculated from the measurements of Lau (1980) cover a much wider range of Δx^+ than the measurements of Kreplin & Eckelmann and do not agree with the physical picture of the wall eddies presented by them. The correlation coefficients were measured as a function of the three spatial coordinates (x^+, y^+, z^+) and time delay τ^+. The origin of the coordinate system ($x^+ = 0$, $y^+ = 0$, $z^+ = 0$) is the projection of the fluid probe on the wall. When $\tau^+ < 0$ the signal from the wall probe leads the one from the fluid probe and vice versa. The correlation coefficients $R_{us_x}(-25, y^+, 0; \tau^+)$ and $R_{ws_z}(-25, y^+, 0; \tau^+)$ calculated for $y^+ = 20$ and 40 are in qualitative agreement with measurements by Kreplin & Eckelmann (1978). The chief difference is that the peaks appear at smaller time delays because the probes are separated in the streamwise direction. The correlation $R_{ws_z}(-25, 40, 0; \tau^+)$ attained negative values during the period $-15 \leqslant \tau^+ \leqslant 2$ and a maximum value of 0.124 at $\tau^+ = 14.7$.

However, as shown in figure 8 the correlation $R_{ws_z}(x^+, 40, 0; 0)$ is negative only for $x^+ = -25$ and is positive for all other values of x^+. When the fluid probe is delayed, negative values appear only at $x^+ = 75$ and $x^+ = 25$. When the wall probe is delayed ($\tau^+ > 0$) R_{ws_z} is positive at all x^+ stations. For the results shown in figure 8 to be consistent with the vortex model it would be necessary for $R_{ws_z}(x^+, 40, 0; \tau^+)$ to be negative for a longer extent in the direction of flow for $\tau^+ \leqslant 0$.

We prefer to interpret these correlation measurements by assuming that the flow at the wall is caused by flow disturbances in the same direction at $y^+ \approx 40$. These disturbances have a convection velocity in the streamwise direction of $C_x^+ \approx 15$ and

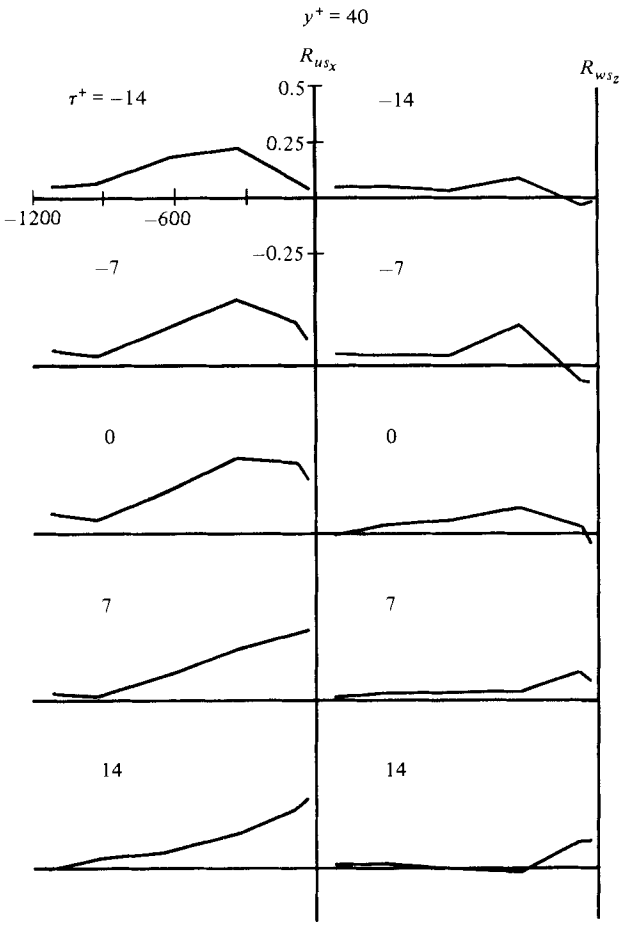

FIGURE 8. Measurements of $R_{us_x}(x^+, 40, 0; \tau^+)$ and $R_{ws_z}(x^+, 40, 0; \tau^+)$.

in a direction normal to the wall of $C_y^+ \approx 2$ at $y^+ = 40$, $C_y^+ \approx 1.5$ at $y^+ = 20$ (Kreplin & Eckelmann 1979). According to this type of interpretation it takes a period of $\Delta T^+ = 20$ for a disturbance to travel from $y^+ = 40$ to the wall. Over this same period the disturbance would be convected downstream a distance of $\Delta x^+ = 300$. Thus it would be expected that large positive or negative transverse flows at $x^+ = 0$, $y^+ = 40$ would be associated with large positive or negative values of s_z at $x^+ = -300$. The observed peak in $R_{ws_z}(x^+, 40, 0; \tau^+)$ shown in figure 8 is consistent with this picture. The correlation coefficient $R_{ws_x}(x^+, 40, 0; \tau^+)$ also shows a peak around $x^+ = -300$ at $\tau^+ = 0$, which moves toward the fluid probe ($x^+ = 0$) for positive time delays.

Correlation measurements of $R_{us_x}(x^+, y^+, 0; \tau^+)$ and $R_{ws_z}(x^+, y^+, 0; \tau^+)$ with $y^+ = 20$ are shown in figure 9. These show a similar behaviour to those for $y^+ = 40$ in figure 8. The only difference is that, for $y^+ = 20$, R_{ws_z} is positive at all x^+ stations for any τ^+ and the peaks at $\tau^+ = 0$ appear closer to the origin. This is consistent with the above physical picture since it takes a shorter time, $\Delta T^+ \approx 13$, for disturbances at $y^+ = 20$ to propagate to the wall.

Measurements of the conditionally averaged streamwise variation of s_z shown in figure 10 are consistent with the correlation measurements. The events that triggered the conditional averaging in figures 6 and 7, an $s_z(z)$ profile at $x^+ = 0$, which indicated a strong positive transverse flow centred at $z^+ = 0$, were used to define $T^+ = 0$. The

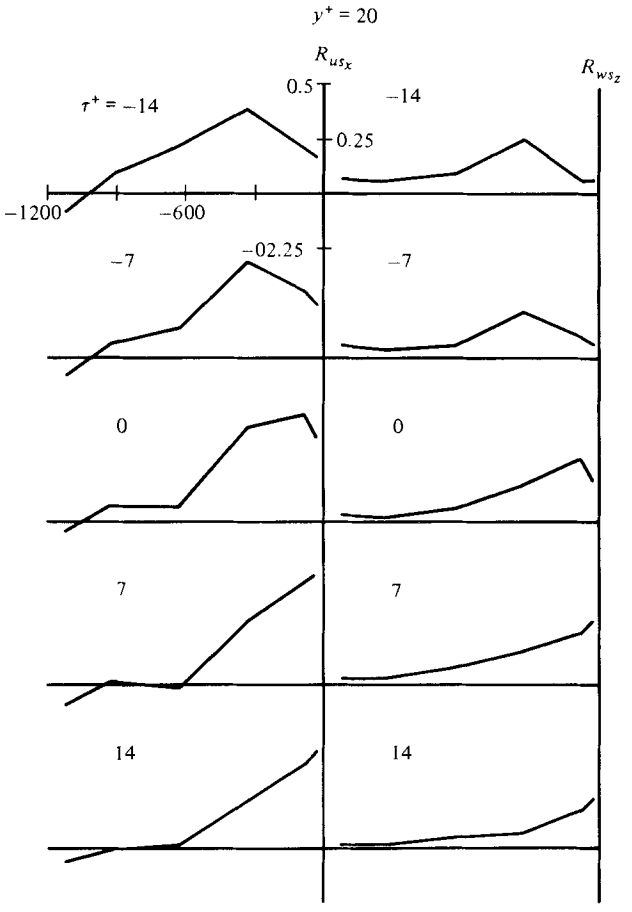

FIGURE 9. Measurements of $R_{us_x}(x^+, 20, 0; \tau^+)$ and $R_{ws_z}(x^+, 20, 0; \tau^+)$.

arrows indicate the magnitude and the direction of the transverse flow either at $y^+ = 20$ or $y^+ = 40$. An arrow length of +750 indicates a value of $\langle w \rangle / (\overline{w^2})^{\frac{1}{2}}$ equal to plus one.

The salient feature of the conditionally averaged $s_z(0, x)$ profiles is the appearance of a peak which, as time progresses, moves to $x^+ = 0$ at a velocity given approximately by $C_x^+ = 15$.

It is seen that a strong transverse flow at the wall at $x^+ = 0$ is on average accompanied by a strong spanwise flow at $y^+ = 20$, $T^+ = -4.2$, $x^+ = -25$ and at $y^+ = 40$, $T^+ = -12$, $x^+ = -25$. As estimated earlier, disturbances at $y^+ = 40$ and $y^+ = 20$ require time intervals of $\Delta T^+ = 20$ and $\Delta T^+ = 13$ to reach the wall. Again, if it is assumed that the convection velocity in the streamwise direction is $C_x^+ = 15$, the maximum in $\langle w \rangle$ at $y^+ = 40$, $T^+ = -12$; $y^+ = 20$, $T^+ = -4.2$ should be accompanied by maxima in s_z at $x^+ = -15 \times 20 = -300$ and at $x^+ = -15 \times 13 = -200$. This is in approximate agreement with the conditionally averaged measurements of $s_z(0, x)$.

The flow reversal at $y^+ = 0$, $T^+ \approx 0$ is not necessarily associated with a reversal of the flow at the wall. There is a hint of a negative flow developing at $x^+ = -325$ for $-2.8 \leqslant T^+ \approx 4.2$, but this is not considered to be conclusive. The spatial variation of w in the spanwise direction at $y^+ = 40$, and not just its direction at a single point, determines the type of wall pattern seen by a fixed observer at the wall. It is necessary

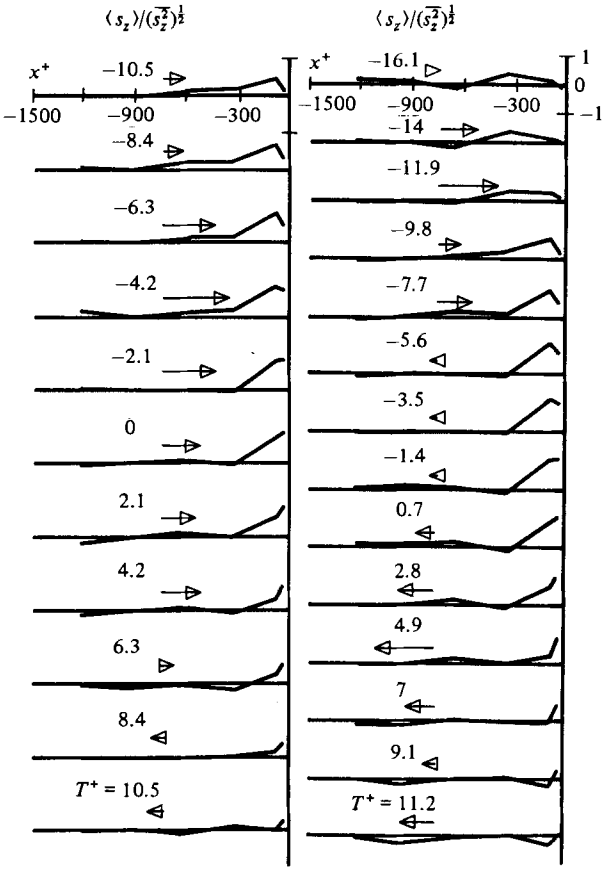

FIGURE 10. Conditionally averaged data for positive transverse flow at the wall; arrows indicate conditionally averaged transverse velocity $\langle w\rangle$ at $y^+ = 40$ (right side of figure) and at $y^+ = 20$ (left side of figure). Arrow length of $+750$ indicates $\langle w\rangle/(\overline{w^2})^{\frac{1}{2}}$ equal to $+1$.

for the flow at $y^+ = 40$ to reverse itself over a sufficient spanwise length in order that the spanwise flow at the wall will change its direction. Therefore, all positive transverse flows at the wall are not necessarily followed by negative transverse flows and vice versa.

4.3. *Coherency normal to the wall*

The correlation coefficients

$$R_{us_x}(-25, y^+, z^+; \tau^+), \quad R_{ws_z}(-25, y^+, z^+; \tau^+), \quad R_{us_z}(-25, y^+, z^+; \tau^+)$$

and

$$R_{ws_x}(-25, y^+, z^+, \tau^+)$$

for $y^+ = 40$ and 20 are shown in figures 11 and 12 respectively. At $y^+ = 40$, R_{ws_z} shows again an interesting behaviour. At zero time delay, the $R_{ws_z}(z^+)$ profile shows a wavelike variation with z^+ which has a wavelength of approximately $\Delta z^+ \approx 90$. Negative values appear around $z^+ = 0$ at $\tau^+ = 0$, but at positive time delays the pattern reverses and positive values appear for all z^+. The wavelength is not so well defined for $\tau^+ > 0$; this is attributed to the fact that there is a certain amount of 'jitter' associated with the wall patterns, as already mentioned in previous sections.

The cross-correlations R_{us_z} and R_{ws_x} are very well defined at $\tau^+ = 0$. They both show a wavelike variation with a wavelength of about 100 wall units and they are

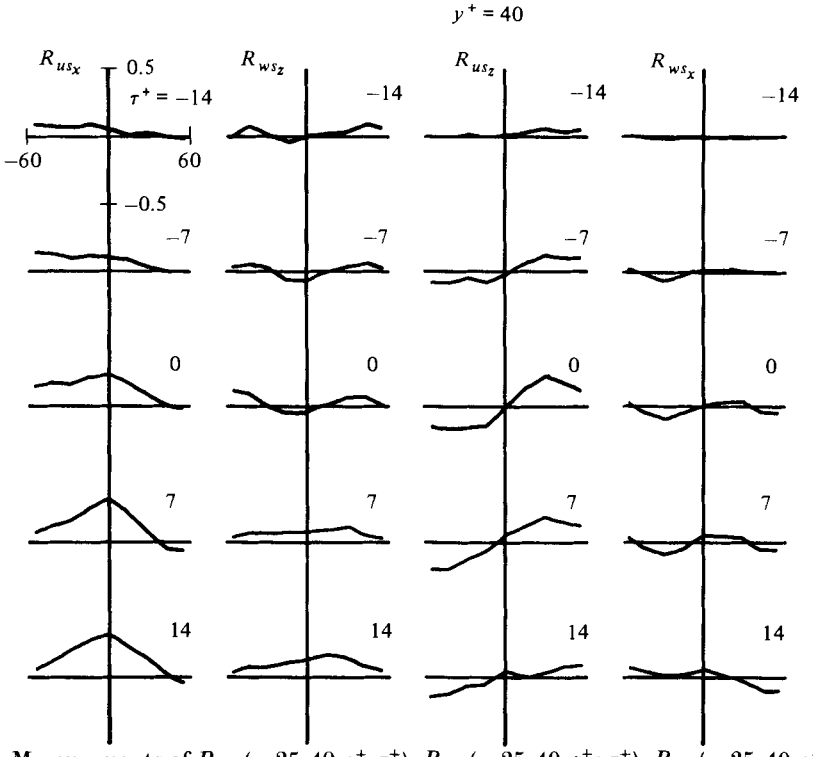

FIGURE 11. Measurements of $R_{us_x}(-25, 40, z^+, \tau^+)$, $R_{ws_z}(-25, 40, z^+; \tau^+)$, $R_{us_z}(-25, 40, z^+; \tau^+)$ and $R_{ws_x}(-25, 40, z^+; \tau^+)$.

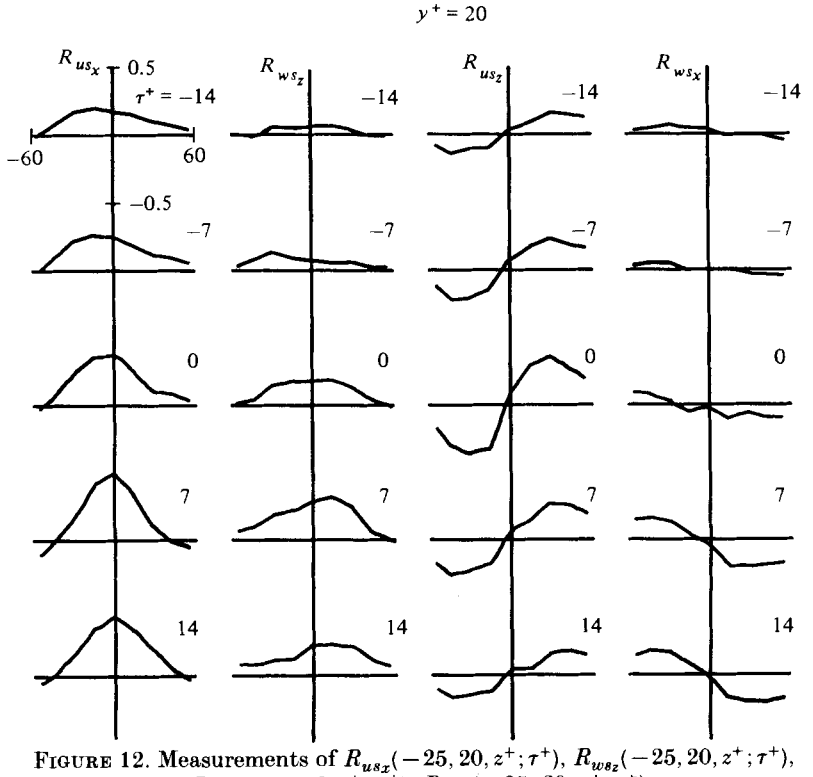

FIGURE 12. Measurements of $R_{us_x}(-25, 20, z^+; \tau^+)$, $R_{ws_z}(-25, 20, z^+; \tau^+)$, $R_{us_z}(-25, 20, z^+; \tau^+)$, $R_{ws_x}(-25, 20, z^+; \tau^+)$.

consistent with the flow picture presented in §4.2. Notice the change in the R_{ws_x} pattern around $\tau^+ \approx 14$, which arises because w reverses direction at $y^+ \approx 40$.

At $y^+ = 20$, the situation is different. The correlation R_{ws_z} is positive for all z^+ and time delays around $\tau^+ = 0$. The correlations R_{us_z} and R_{ws_x} are again well-defined wavelike patterns, and the differences in the R_{ws_x} pattern, from what was obtained with the probe at $y^+ = 40$, arises because w is in phase with the flow at the wall.

All the correlation coefficients are in agreement with the flow model presented in §4.2. In particular, the cross-correlation coefficients show a behaviour that is similar to the one obtained at the wall. The present measurements agree well with measurements obtained by Lee *et al.* (1974) using only wall probes (note that $R_{us_z}(-25, y^+, z^+; 0)$ is analogous to $R_{s_x s_z}(0, 0, z^+; 0)$ at the wall), supporting the assumption of coherency up to $y^+ = 40$.

Any conclusion about the wavenumber variation of w at $y^+ = 40$ or 20 is not possible since the calculation of a correlation coefficient involves some sort of filtering (spatial filtering in this case). There is an indication that a wavelength selection occurs whose details are still unknown, and there is a definite need for an elucidation of this process.

5. Concluding remarks

Measurements of the streamwise and spanwise components of both the velocity gradient at multiple wall locations and the velocity at single points in the fluid were performed. Conditional-averaging techniques were used to relate the wall structures to phenomena occurring in the fluid. On the basis of these experiments, an eddy model is proposed which is believed capable of accounting for the most important features of the flow in the viscous wall region.

Strong spanwise flows at the wall are closely associated with strong spanwise flows at $y^+ = 40$ and 20 that have the same direction and occur at an earlier instant in time. Since the fluid at the wall does not respond immediately to changes at $y^+ = 40$, and since the velocity field changes in the x-direction a description of the wall structures requires that an account must be taken of the finite times needed for a disturbance to propagate in the direction of flow and towards the wall.

Consequently a characteristic feature of the flow field is the reversal of the spanwise flow at $y^+ = 40$ during the time that a strong spanwise flow occurs at the wall. At $y^+ = 20$ the conditionally averaged spanwise velocity leads, but always has the same phase as, the flow at the wall.

Measurements of conventional correlation coefficients as a function of the three spatial coordinates and time are consistent with the above flow model. In addition they provide support for the notion that the flow is coherent from the wall out to $y_0^+ \approx 40$.

Various other eddy models, which attempt to account for the kinematics of the viscous wall region, have been proposed in the literature. Prominent among these is the suggestion that the flow is dominated by counterrotating vortices, whose length in the flow direction is of the order of $\Delta x^+ \approx 1200$. Their extent in the direction normal to the wall doesn't seem to be well defined, but conventional correlation measurements and conditionally averaged measurements suggest that the eye of such vortices would not move, on average, below $y^+ \approx 20$–30. These vortices are visualized to be 'pumping' low-momentum fluid away from the wall and thus influencing the streamwise velocity field.

The results presented in this paper, as well as in previous papers published from

this laboratory, agree with this model in that they support the notion that wall structures transfer negative-momentum fluid away from the wall and thus influence the dynamics of the flow in the streamwise direction. However, our present measurements are not in agreement with other aspects of the vortex model in that we find spanwise flow patterns at the wall to be caused by flow deviations outside the viscous wall region that are in the same direction. The appearance of streamwise vortical structures is considered to be a consequence of the lag time for a spanwise disturbance to travel from $y^+ \approx 40$ to the wall.

According to the flow model used in this paper the streamwise extent of this 'vortical' structure should be $\Delta x^+ \approx -300$. If it is assumed that a spanwise disturbance originates at $y^+ = 40$, $x^+ \approx -300$ and $T^+ = 0$ and travels both downstream and towards the wall, then it reaches $x^+ \approx 0$, $y^+ = 40$ and $x^+ \approx -300$, $y^+ = 0$ at about the same time ($T^+ \approx 20$). The flow at the wall at $x^+ \approx 0$, $T^+ \approx 20$ will, on average, be in the opposite direction, having been caused by a spanwise flow that occurred earlier in time. So when the flow changes directions at $x^+ = 0$, $y^+ = 40$ and $T^+ \approx 20$, the flow at the wall is expected to be in the opposite direction for $-150 \leqslant x \leqslant 150$, which is consistent with the results of figure 9.

Blackwelder & Eckelmann (1979) used a conditional averaging scheme that is triggered by a sharp acceleration of the flow in the streamwise direction following a streamwise momentum deficient flow at $y^+ = 15$. Their results differ from the results presented in this paper in a number of ways and this could partially account for their different viewpoint on the wall eddies. The wavelength of their wall patterns is not very well defined and there is a loss of correlation at $z^+ = 34$, especially with the $\langle u \rangle$ velocity profile. Their measurements of $\langle w \rangle$ at $y^+ = 40$ don't show the characteristic signature of the spanwise component of the velocity that our measurements revealed; that is, a flow reversal, with the return flow having the same magnitude as the flow that preceded it in time.

Their measurements, especially at $z^+ = 34$, would also imply that a vortical structure appears as a suddenly spinning mass of fluid and not because of the lag time between flow changes at $y^+ \simeq 40$ and $y^+ = 0$. We believe that these differences arise because the detection scheme used by Blackwelder & Eckelmann has the disadvantage, already pointed out in §1, that a single fixed detection probe does not use information regarding the spatial development of the patterns under investigation.

It is also our contention that the event that triggered the conditional-averaging scheme used by Blackwelder & Eckelmann is just one aspect of the evolution of the coherent structures in the wall region. Consequently they were not able to focus sharply on the spanwise variations in w or s_z that give evidence of flow-oriented wall eddies.

This work is supported by the Office of Naval Research under Grant NR 062-558.

REFERENCES

BAKEWELL, H. P. & LUMLEY, J. L. 1967 *Phys. Fluids* **10**, 1980.

BLACKWELDER, R. F. & ECKELMANN, H. 1978 In *Structure and Mechanisms of Turbulence I (ed. H. Fiedler). Lecture Notes in Physics, vol.* 75, *p.* 190. *Springer.*

BLACKWELDER, R. F. & ECKELMANN, H. 1979 *J. Fluid Mech.* **94**, 577.

CHORN, L. G., HATZIAVRAMIDIS, D. T. & HANRATTY, T. J. 1977 *Phys. Fluids Suppl.* **20**, S112.

CORRSIN, S. 1957 In *Proc. Symp. on Naval Hydrodynamics, Publ.* 515, NAS-NRC 373.

FORTUNA, G. 1971 Ph.D. thesis, University of Illinois, Urbana.

HATZIAVRAMIDIS, D. T. & HANRATTY, T. J. 1979 *J. Fluid Mech.* **95**, 655.

HOGENES, J. H. A. 1979 Ph.D. thesis, University of Illinois, Urbana.

HOGENES, J. H. A. & HANRATTY, T. J. 1982 *J. Fluid Mech.* **124**, 363.

KAPLAN, R. E. & LAUFER, J. 1969 In *Proc. 12th Intl Congr. Appl. Mech., Stanford*, p. 236. Springer.

KLINE, S. J., REYNOLDS, W. C., SCHRAUB, F. A. & RUNSTADLER, P. W. 1967 *J. Fluid Mech.* **30**, 741.

KLINE, S. J. & RUNSTADLER, P. W. 1959 *Trans. A.S.M.E.* E: *J. Appl. Mech.* **26**, 166.

KOVASZNAY, L. S. G., KIBENS, V. & BLACKWELDER, R. F. 1970 *J. Fluid Mech.* **41**, 283.

KREPLIN, H. P. & ECKELMANN, H. 1979 *J. Fluid Mech.* **95**, 305.

LAU, K. K. 1980 Ph.D. thesis, University of Illinois, Urbana.

LEE, M. K., ECKELMANN, L. D. & HANRATTY, T. J. 1974 *J. Fluid Mech.* **66**, 17.

RUNSTADLER, P. W., KLINE, S. J. & REYNOLDS, W. C. 1963 *Dept Mech. Engng, Stanford University, Rep.* MD-8.

SIRKAR, K. K. 1969 Ph.D. thesis, University of Illinois, Urbana.

SIRKAR, K. K. & HANRATTY, T. J. 1970*a* *J. Fluid Mech.* **44**, 589.

SIRKAR, K. K. & HANRATTY, T. J. 1970*b* *J. Fluid Mech.* **44**, 605.